High efficiency blue and green light-emitting diodes using ruddlesden–popper inorganic mixed halide perovskites with butylammonium interlayers

Vashishtha, Parth; Ng, Michael; Shivarudraiah, Sunil B.; Halpert, Jonathan E.

2018

Vashishtha, P., Ng, M., Shivarudraiah, S. B., & Halpert, J. E. (2018). High Efficiency Blue and Green Light-Emitting Diodes Using Ruddlesden–Popper Inorganic Mixed Halide Perovskites with Butylammonium Interlayers. Chemistry of Materials, 31(1), 83–89. doi:10.1021/acs.chemmater.8b02999

https://hdl.handle.net/10356/143893

https://doi.org/10.1021/acs.chemmater.8b02999

CHEMISTRY OF MATERIALS
Cite This: Chem. Mater. 2019, 31, 83−89
Article
pubs.acs.org/cm

High Efficiency Blue and Green Light-Emitting Diodes Using Ruddlesden−Popper Inorganic Mixed Halide Perovskites with Butylammonium Interlayers

Parth Vashishtha,[†,§] Michael Ng,[‡] Sunil B. Shivarudraiah,[‡] and Jonathan E. Halpert*[,†,‡]

[†]MacDiarmid Institute for Advanced Materials and Nanotechnology, and School of Chemical and Physical Sciences, Victoria University of Wellington, P.O. Box 600, Wellington, New Zealand

[‡]Department of Chemistry, Hong Kong University of Science and Technology (HKUST), Clear Water Bay Road, Kowloon, Hong Kong

[§]School of Materials Science and Engineering, Nanyang Technological University (NTU), 50 Nanyang Avenue, Singapore 639798, Republic of Singapore

Supporting Information

ABSTRACT: Ruddlesden−Popper phase inorganic metal halide perovskites are promising candidates for efficient light-emitting diodes (LEDs) with high brightness and color purity. Here, we demonstrate LEDs made from in situ grown $CsPbX_3$ quasi 2D/3D thin films that are color tunable across the entire visible spectrum. $CsPbX_3$ nanosheets are used to produce RP phase perovskites using butylammonium as a separating ligand to create $BA_2Cs_{n-1}Pb_n(Br/Y)_{3n+1}$ 2D/3D mixed halide thin films, where Y = Cl or I. The number of $CsPbBr_3$ monolayers in these crystals was optimized by changing the butylammonium concentration. We demonstrate a stable perovskite phase with thin emission line widths providing points covering the edge of the CIE triangle and a maximum red/green/blue coverage of ∼130% of the National Television System Committee color standard. Additionally, we are able to report record efficiencies for blue emitting perovskite nanocrystal LEDs with a maximum external quantum efficiency (EQE) of 2.4% and 6.2% at 465 and 487 nm and a maximum luminance of 3340 cd/m^2. We also demonstrate efficient green LEDs with a maximum efficiency of 10.1% EQE, 23.3 cd/A and 9.8 lm/W at 16.3 mA/cm^2.

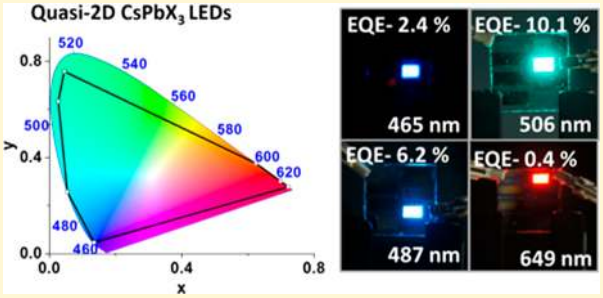

INTRODUCTION

Inorganic metal halide perovskite light emitting devices have gained significant attention due to their low trap density, composition and color tunability, and high PL quantum yield.[1−5] Perovskite colloidal nanocrystals (NCs) have shown high quantum yield (QY), but the external quantum efficiency (EQE) and stability of these light-emitting diodes (LEDs) suffer due to their bulky organic ligands and surface defects.[2,6,7] Alternatively, 3D bulk metal halide perovskites have been found to display relatively less narrow emission spectra and less color tunability across the visible spectrum.[7,8] 2D perovskite LEDs have promising color purity and luminance but were also found to be inefficient due to a larger exciton binding energy than 3D perovskites, a result of geometric and dielectric contrast effects.[9−11] For all these materials, the challenge remains the same: making stable and efficient LEDs with high brightness and color purity that can rival cadmium based quantum dot LEDs (QDLEDs).[12−15]

To overcome these issues, one solution is to use quasi-2D perovskite materials made from relatively thick RP phase 2D perovskites.[1,16−20] The use of thicker nanosheets weakens the binding energy of the excitons and thus can combine the color purity and tunability of 2D structures with the conduction properties of 3D crystals.[9,11,21] Here we report a Ruddlesden−Popper (RP) phase perovskite of roughly 15−30 monolayers with the formula is $A'_2A_{n-1}Pb_nX_{3n+1}$, where A′ is a large ammonium organic cation, A is the monovalent inorganic cation (Cs^+) and X is a halogen (Cl, Br, I). In the RP perovskite structure, the larger bandgap organic cation works as an insulating layer or a barrier between $(PbI_6)^{2-}$ octahedra on either side of the interface between 2D crystals of $CsPbX_3$. The optical properties can be tuned by either mixing the halide anions (X = I/Br or Br/Cl) or by changing the number of inorganic perovskite layers (n) between the large organic cation (A′) to alter the degree of excitonic confinement in each nanosheet.[9,19] Using organic A′ groups as separation layers in quasi-2D films has permitted significant improvement recently in the moisture stability in $MAPbX_3$ perovskite LEDs and in solar cells.[7,22−24] Furthermore, organic hybrid perovskites have been used to produce reasonably efficient green and red

Received: July 16, 2018
Revised: November 25, 2018
Published: November 26, 2018

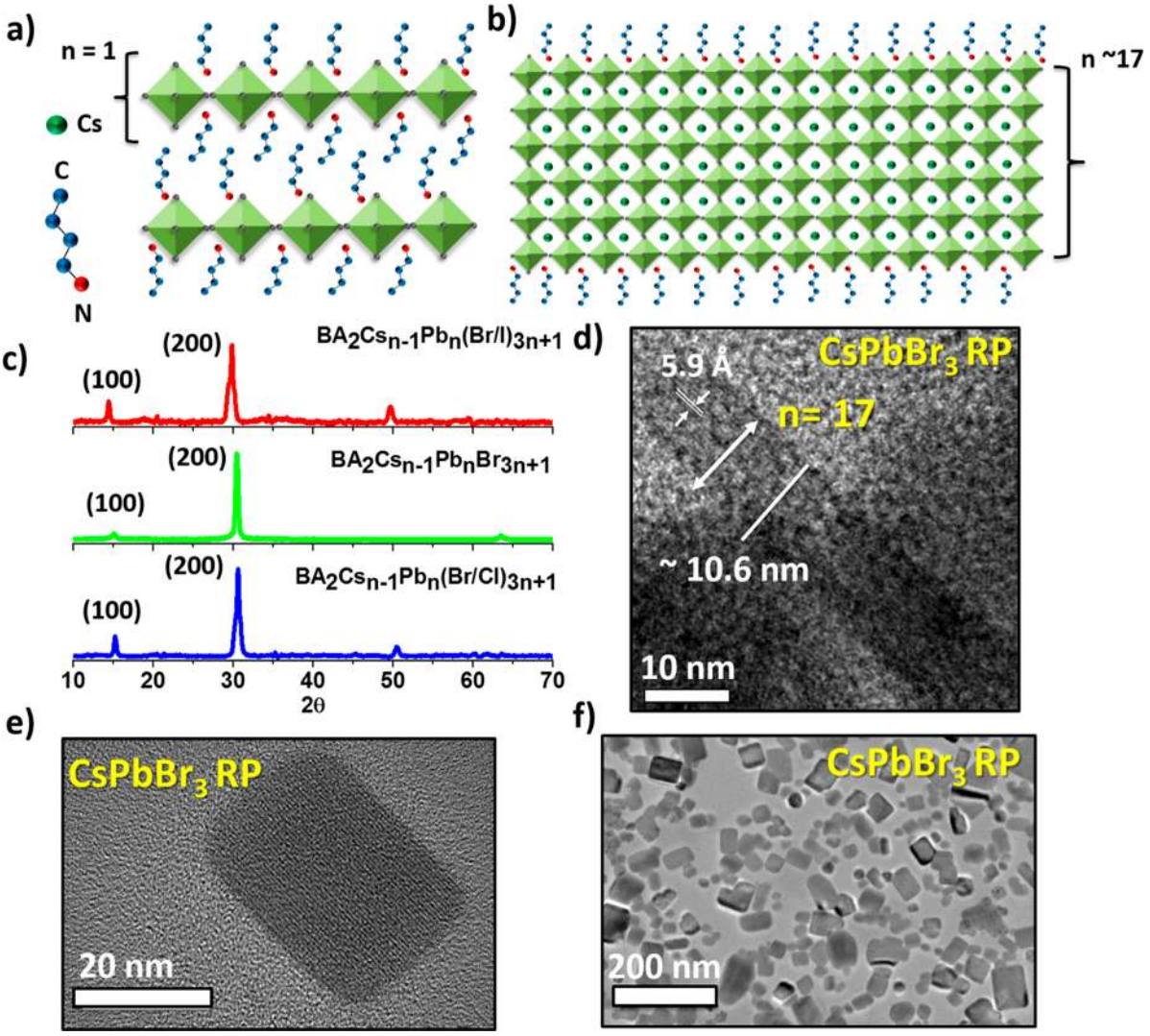

Figure 1. Illustrated structure of $BA_2Cs_{n-1}Pb_nX_{3n+1}$ RP perovskites for (a) thin (n = 1) (b) and thick nanosheet layers. (c) XRD spectra of $BA_2Cs_{n-1}Pb_n(Br/Y)_{3n+1}$, Y = Cl or I. Perovskite thin films were spin coated onto PVK and PEDOT:PSS for the XRD measurements. Low angle XRD peaks (2θ < 10) were absent as n was larger than 16 in these RP perovskite thin films. Panels d, e and f show TEM images of the $BA2Cs_{n-1}PbnBr_{3n+1}$ RP perovskites after removal from the substrate. Panel d shows a high resolution TEM image where number of planes can be observed in the material from a side view of a single nanosheet.

emitting LEDs.[16−19] To date, Si et al. produced pure inorganic $CsPbBr_3$ and $CsPbI_3$ perovskites in the RP phase for red LEDs, using phenylbutylammonium as the A′ group,[16] but there is as of yet no report on precise color tuning in cesium based RP perovskite LEDs.[25,26] Additionally, blue perovskite LEDs have lagged behind green LEDs in both EQE and luminance.[25,27] Whereas pure $CsPbBr_3$ emits in the green with high quantum yield, blue LEDs require precise tuning of the band gap and efficient blue LEDs are generally more difficult to produce.[15,25]

Here, we demonstrate in situ grown, pure inorganic nanosheets of $CsPb(X/Y)_3$ [X/Y = I/Br or Br/Cl] using butyl ammonium (BA) as the A′ group in an RP phase and mixed halides X/Y to tune the color of emission in addition to color tuning by layer thickness.[18,28,29] The chemical formula of the nanostructured perovskite layers is thus $BA_2Cs_{n-1}Pb_n(Br/X)_{3n+1}$ [X = Cl, I]. We demonstrate efficient, pure color LEDs in the blue and green (BG), along with inefficient but pure color red (R) LEDs, with the EL emission tunable from 465 to 680 nm.

LEDs in the blue region show peak EQEs of 2.4% and 6.2% at 465 and 487 nm peak electroluminescence wavelengths, respectively, and represent the best recorded blue perovskite LEDs to date (Table S2).[30−33] The best overall EQE for these devices was 10.1% for a blue-green device emitting at 506 nm.

RESULTS AND DISCUSSION

The RP perovskite films were prepared by spin coating the precursor solution, which consists of (BA)Br, $PbBr_2$ and CsBr dissolved in DMSO, onto PEDOT:PSS and PVK coated, patterned ITO/glass. Color tuning was achieved by changing the halide mixture and altering the BA concentration to achieve the desired photoluminescence peaks and optimal external quantum efficiency (EQE).[34]

Figure 1a shows a schematic diagram of an RP perovskite crystal structure. Here the $(PbI_6)^{2-}$ octahedra are separated from each other by the butylammonium (BA) organic cations, forming a layered structure. The butylammonium cation is a larger bandgap material that gives rise to a quantum well-like structure in the thin film as successive 2D layers stack on top of

DOI: 10.1021/acs.chemmater.8b02999
Chem. Mater. 2019, 31, 83−89

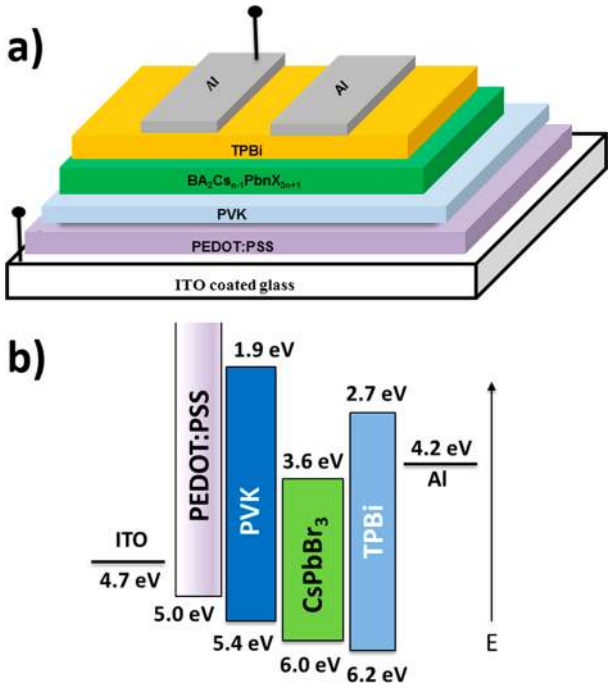

Figure 2. (a) Device schematic and (b) energy diagrams for the ITO/PEDOT:PSS/PVK/$CsPbBr_3$ RP pero/TPBi/Al LEDs.[36−38]

one another. Figure 1a is an illustration of a pure 2D structure with only one layer (n = 1) and contains no cesium ions. Figure 1b shows a schematic diagram for a quasi 2D perovskite similar to the one depicted in the HRTEM measurements (n = 17 ± 3). There, inorganic layers are formed such that the BA organic cation connects the terminal octahedra of one nanosheet to those of the next. If the number of planes is infinite, then the layered structure becomes a 3D crystal. In Figure 1c, the XRD spectrum confirms the formation of the perovskite structure. The pure $CsPbBr_3$ XRD spectrum shows the diffraction peaks at 15.1° and 30.4°, which correspond to the (010) and (020) planes of perovskite NCs.[16] A similar trend was observed in the mixed halide; however, the diffraction peak was shifted toward lower angles in the case of bromide-iodide mixed halides and toward a higher angle for bromide-chloride mixed halide perovskites. Lower angle diffraction peaks consistent with phase pure, thin nanosheets are not expected to be observed because the number of planes was higher than 16, on average.[16] In order to extract the nanosheets from the substrate on which they were grown, chloroform was used to disperse the nanosheets and dissolve the underlying organic layers. Figure 1d shows the high resolution TEM image of these nanosheets, which illustrates the lattice fringes with d spacings of 5.9 Å and a thickness of n = 17 ± 3 monolayers. Figure 1e,f shows the TEM images of the extracted $CsPbBr_3$ perovskite NCs, which confirm the

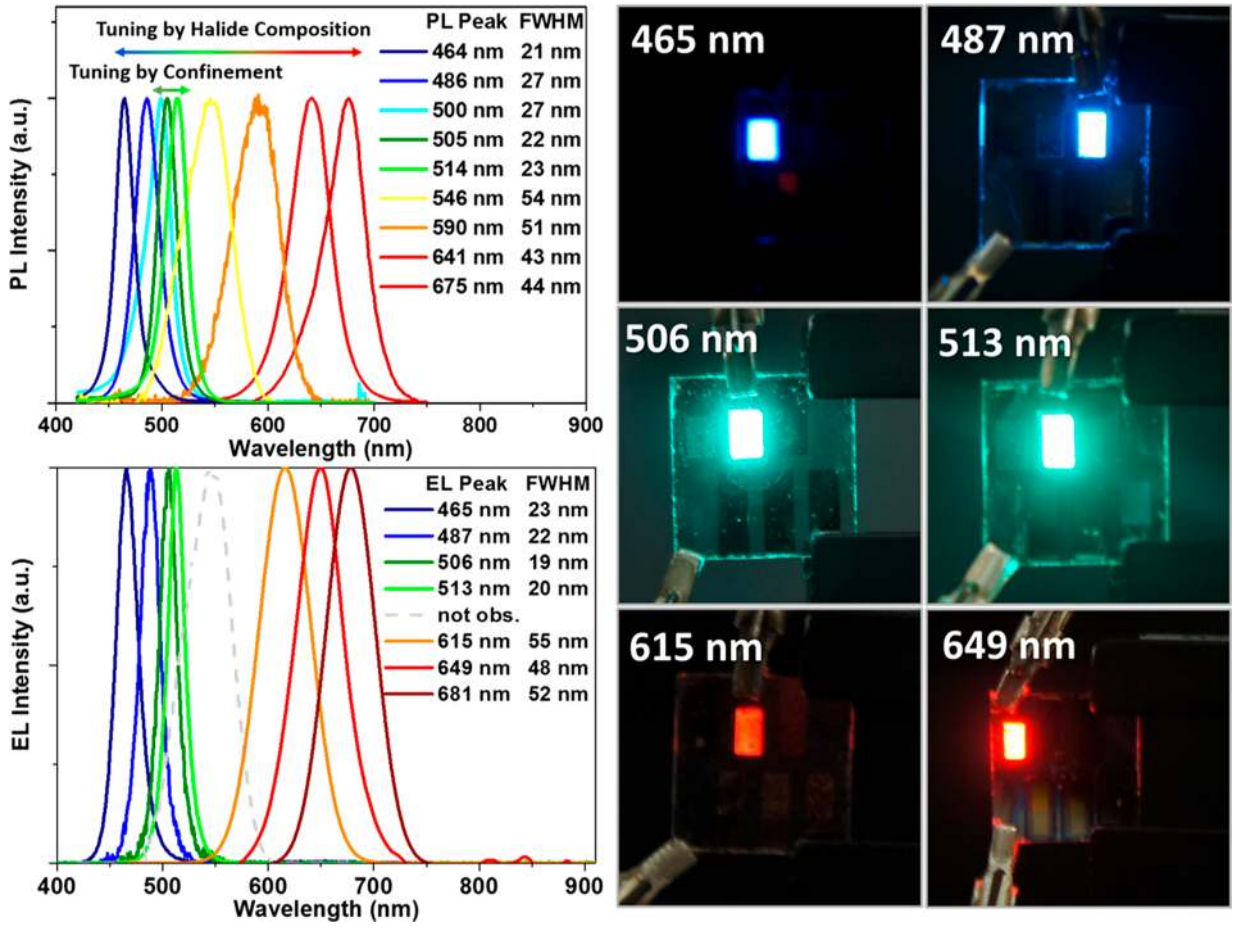

Figure 3. Normalized PL spectra (top) at 400 nm excitation of $CsPb(Br/Y)_3$ RP perovskite thin films in device, normalized EL spectra (bottom left) of the same devices at the turn-on voltage. Unprocessed photos of these LEDs (right). Color tuning was achieved by taking advantage of the confinement effect as well as halide mixing.

DOI: 10.1021/acs.chemmater.8b02999
Chem. Mater. 2019, 31, 83−89

Table 1. PL and EL Matrices for RP Perovskite LEDs[a]

LED label	Br:Y ratio	PL peak[35]	EL peak[35]	V_t (V)	EQE_{max} (%)	EL at EQE_{max} (%)	Luminance at EQE_{max} ($cd \cdot m^{-2}$)
B465	0.42:0.58	464	465	5.0	2.4	467	962
B487	0.84:0.16	486	487	4.5	6.2	487	3340
G506	1.0:0	505	506	4.5	10.1	506	3810
G513	1.0:0	514	513	4.5	7.2	513	11200
Y546	0.70:0.30	546	654	8.0	0.69	654	1070
O615	0.60:0.40	590	615	4.0	0.41	625	313
R649	0.45:0.55	641	649	4.0	0.13	655	18.5
R681	0.10:0.90	675	681	4.0	0.08	678	5.6

[a] V_t is turn-on voltage, Y is Cl or I, G513 has 0.5× the standard BA concentration (see Table S2).

formation of quasi-2D nanosheets. The mean number of planes (n) for this sample is estimated to be ~24 ± 7 monolayers. As the number of planes increases, with decreased BA concentration, the emission peak moves toward higher wavelengths (Figure S1).

LEDs were fabricated from ~50 nm thick thin films of the RP phase perovskite (see Methods for complete details) deposited onto PEDOT:PSS and PVK, which act as the hole transport layers. Devices were completed by thermally evaporating TPBi as an electron transport layer, and a patterned Al electrode was thermally evaporated via shadow masking for an active area of 6 mm^2 per device. In the case of $BA_2Cs_{n-1}Pb_n(Br/I)_{3n+1}$ LEDs, a poly-TPD layer was first coated onto PEDOT:PSS at 3000 rpm and then a thin layer of about 5 nm of PVK was deposited.[16,38] The device structure and literature band values for all layers are shown in Figure 2.[36−38] The current density−voltage ($J-V$) curves for all the devices are shown in Figure S3.

Figure 3 (left) shows the unprocessed photographs of LEDs at their turn-on voltages (4.0−5.0 V). Photoluminescence[34] peaks in the thin film and their corresponding EL peaks are recorded at their turn-on voltages as shown in Figure 3 (right). The PL peak position of the B506 device is at 505 nm, which is 22 nm blue-shifted from that of the bulk $CsPbBr_3$. This suggests a significant degree of confinement in films synthesized using a high BA concentration.[39] The PL and EL peak position and fwhm are very close in value, except again for the Y546 device, which performed poorly to ion mobility effects.[38] The performance metrics for all devices are listed in Table 1. Red LEDs were found not to be as efficient and stable as the blue and green LEDs, due to ion migration effects.[40,41] $CsPb(Br/I)_3$ LEDs with high bromide content, in particular, were found to be highly color unstable due to an extreme ion migration effect, a phenomena also previously observed in perovskite NCLEDs.[38] Devices with high iodide content were found to be more color stable but showed very low EQE, due to the phase instability of the $CsPbI_3$ crystal structure.[42] It should be noted that researchers have shown high EQEs of 7% in pure $CsPbI_3$ RP perovskite LEDs, but that stable mixed halide devices have yet to be observed,[16] as was the case here. The blue LEDs, emitting at 465 and 487 nm, were found to red-shift slightly at higher voltages (>8.5 V) but had stable CIE points at low voltage. Pure $CsPbBr_3$ LEDs, emitting at 506 and 513 nm, and color tuned via nanosheet thickness, were found to be color stable with no EL shift, even at high bias (>9.0 V). Figure 4 shows the change in the EQE (panel a), luminance (panel b), current efficiency (panel c) and luminous efficacy (panel d) with voltage for blue and green LEDs. In all these devices, the efficiency increases rapidly after their turn-on voltages and drops off after 8 V. B486 shows the highest EQE for a blue perovskite LED of 6.2% with a luminance of 3340 cd/m^2 at 8.0 V. G506 has shown the highest EQE for this device type with an EQE of 10.1% at 7.5 V and a maximum luminance of 8740 cd/m^2, just below the best green perovskite LEDs to date.[19] G513 displayed an EQE of 7.2% with 11 200 cd/m^2 luminance at 8.5 V. Efficiency roll-off at high current density was also observed for most devices (see Figure S4). However, green devices were found to be stable running for 75 min under ambient conditions without packaging. Under these conditions, 75% of the device EQE value was retained for B506 for the first 45 min of the operation period at constant current density (see Figure S5). The red LEDs displayed EQEs of less than 0.5% and are described in more detail in Figure S7 of the Supporting Information. The turn-on voltage was found to be between 4.0 and 5.0 V except for device Y546, where the device was found to be turn on at 8.0 V. The EQE was also found to be low in this device with a huge color shift due to ion migration in the active layer (Figure S7). Similar behavior has been observed previously in mixed halide $CsPb(Br/I)_3$ perovskite LEDs emitting in this region.[38]

Figure 5 shows the CIE diagram of all the investigated LEDs, showing the color tunability in the entire visible spectrum for in situ grown RP perovskites. The thin line widths of emission at 465, 518 and 640 nm gives points at the far edges of the diagram. Compared with the National Television Standard Committee (NTSC) color triangle, the red/green/blue (RGB) color triangle of the RP perovskite LEDs shown here is 30% larger.[43]

In conclusion, we have shown the color tunability in $BA_2Cs_{n-1}Pb_n(Br/X)_{3n+1}$ [X = Cl, I] RP phase perovskite LEDs using BA as an organic cation and by mixing the constituent halide anions. The number of planes in the 2D nanosheets of $CsPbBr_3$ were found to be around ~24 ± 7 for optimal performance in LEDs emitting at 505 nm. This quasi-2D/3D material balances the thin emission line width and high QY of thin nanosheets with the superior conduction properties of thicker perovskite crystals. We have also shown record EQEs in the blue spectral region, which outperforms the current literature values for blue RP perovskite LEDs. The tuning in the green emission spectra is shown by varying the BA amount in pure $CsPbBr_3$ and these devices were found here to have a maximum EQE of 10.1%.

While the ion migration issue is yet to be completely resolved for mixed Br/I perovskites, red LEDs were also achieved with this material set. Finally, these results show that mixed 2D/3D materials can be tuned for very high performance in the critical blue and green spectral regions.

DOI: 10.1021/acs.chemmater.8b02999
Chem. Mater. 2019, 31, 83−89

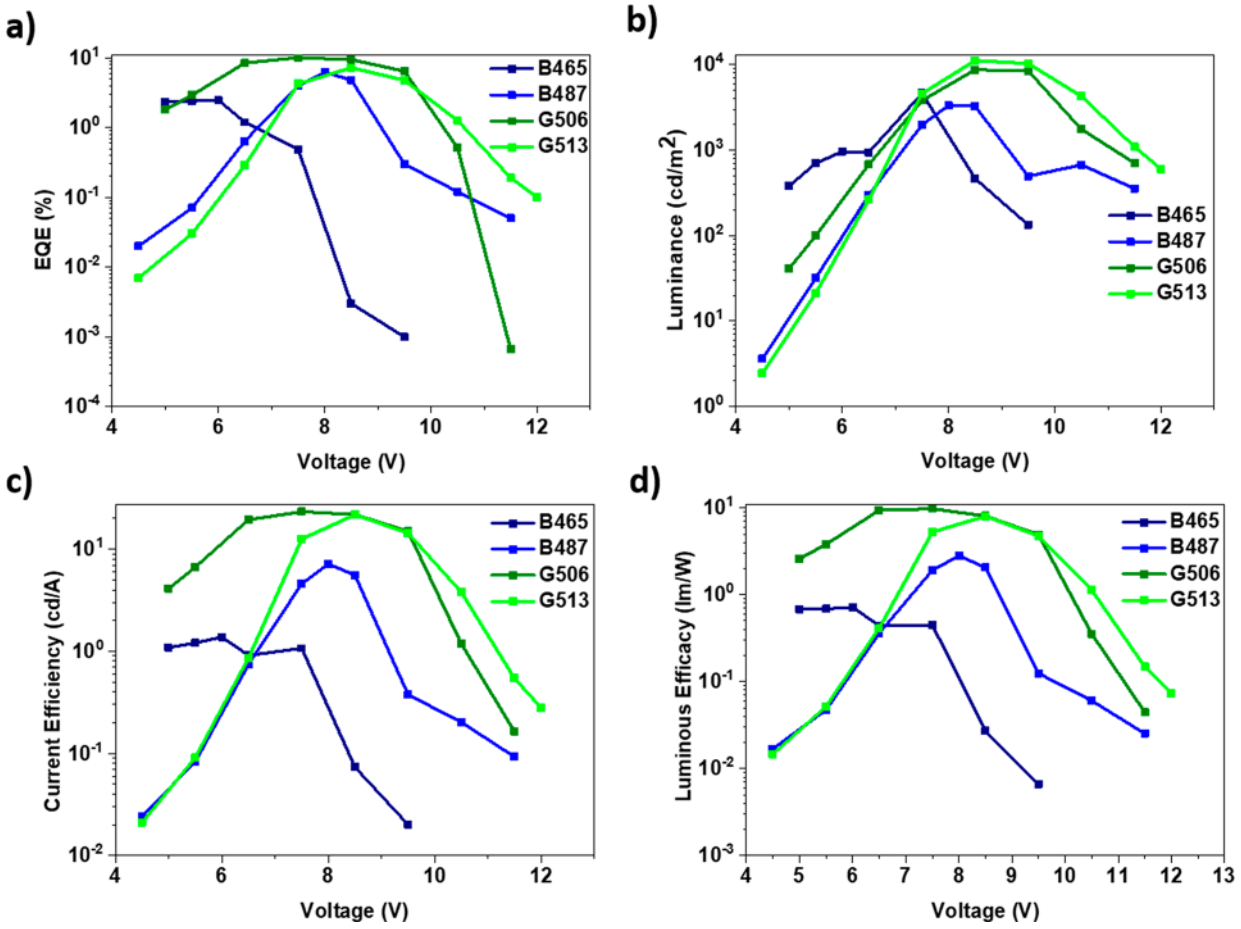

Figure 4. Plots of (a) EQE, (b) luminance (cd·m^2), (c) current efficiency (cd/A) and (d) luminous efficacy (lm/W) vs voltage for B465, B487, G506 and G513 (blue and green) LEDs for champion devices. Device statistics are shown in Table S4.

EXPERIMENTAL SECTION

PVK LT-N4077 (MW > 20 000 g mol^{-1}), TPBi LT-E302 (MW = 654.76 g mol^{-1}), were purchased from Lumtec. PEDOT:PSS (AL4083) was purchased from Ossila. *N*-Butylammonium bromide and *n*-butyl ammonium iodide were purchased from GreatCell Solar. Cesium bromide, cesium iodide, lead(II) chloride, lead(II) bromide, lead(II) iodide, anhydrous dimethyl sulfoxide (DMSO), anhydrous *m*-xylene and anhydrous chlorobenzene were purchased from Aldrich.

Perovskite precursor solution was prepared by mixing *n*-butylammonium bromide, lead bromide and cesium bromide in DMSO. Precise ratios of bromide, chloride and iodide precursors were mixed to synthesize mixed halide precursor solutions (see Table S1 for details).

Devices were fabricated by spin coating PEDOT:PSS, PVK and perovskite precursor solutions, followed by thermal evaporation of the TPBi electron transport layer and the Al electrode. For $CsPb(Br/I)_3$ LEDs, poly-TPD was spin coated on top of PEDOT:PSS and then a very thin layer of PVK was spin coated at 4000 rpm on top of poly-TPD to improve the adhesion of the perovskite film. The perovskite layer was spin coated as described above (see Figure S8 for details).

A Carry 50 UV−visible spectrophotometer was used for UV−vis absorbance measurements and a Horiba Fluorolog-3 Spectrometer was used for PL measurements. Thin film photoluminescence quantum yield (PLQY) measurements were obtained using a Quanta-phi integrating sphere connected to a Horiba Fluorolog system via optical fiber bundles. A 400 nm excitation wavelength was used, with a bandpass slit width of 1 nm for excitation and emission, which corresponds to a rough power density of from 10^{-5} to 10^{-6} W/m^2. A Jeol 2100 was used for HRTEM analysis. X-ray diffraction patterns were recorded by a PANalytical X-ray diffractometer using Cu Kα radiation, an 45 kV operating voltage and 40 mA current.

A Keithley 236 SMU instrument was used as a power source for the LED. All the LEDs were characterized in ambient condition using a QE Pro Ocean Optics spectrometer connected with a 200 μm optical fiber (QP200-2VIS-NIR). The fiber was carefully calibrated with an Ocean Optics HL-3 plus VIS-NIR light source and a Lambertian profile was assumed to compute the total spectral flux for the EQE calculation (see SI for further details).

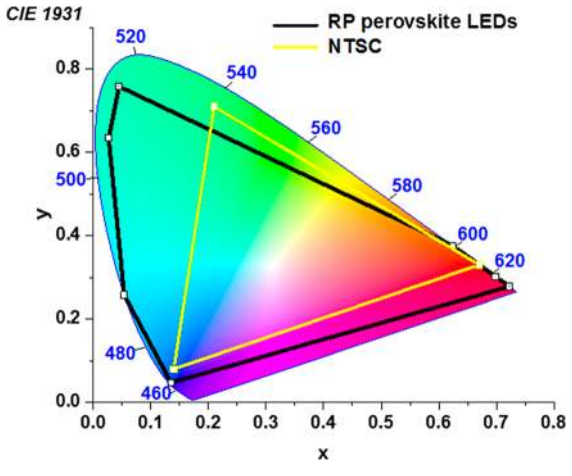

Figure 5. CIE chromaticity coordinate diagram for the $CsPbX_3$ RP perovskite LEDs at their turn-on voltages.

DOI: 10.1021/acs.chemmater.8b02999
Chem. Mater. 2019, 31, 83−89

■ ASSOCIATED CONTENT

Supporting Information

The Supporting Information is available free of charge on the ACS Publications website at DOI: 10.1021/acs.chemmater.8b02999.

Additional TEM micrographs of RP perovskite nanosheets, a chart showing emission over time for this device type, a chart of efficiency vs current density in blue-green devices, a chart of EL peak position over different voltage in LEDs, a chart of efficiency vs voltage in red LEDs, absorption spectra of RP perovskite thin films, PL spectra of RP perovskite thin film with varying the BA concentration, and PLQY measurements on a selection of thin films (PDF)

■ AUTHOR INFORMATION

Corresponding Author

*Jonathan E. Halpert. E-mail: jhalpert@ust.hk.

ORCID

Parth Vashishtha: 0000-0002-3712-8177

Jonathan E. Halpert: 0000-0002-9499-2658

Author Contributions

All experimental work was provided by P.V. with the exception of the PLQY experiments in the SI. The PLQY measurements, Tables S5 and Figure S10 were provided by M.N. and S.B.S. All other figures and analysis were provided by J.E.H. and P.V. who both contributed to the paper preparation.

Funding

J.E.H. and P.V. acknowledge the Royal Society of New Zealand for funding under the Marsden Fund via Grant E2646/3416. J.E.H. also acknowledges funding from the Rutherford Discovery Fellowship via Grant E2675/2990. J.E.H. also recognizes funding from HKUST via projects N1758 and R9398.

Notes

The authors declare no competing financial interest.

■ ACKNOWLEDGMENTS

We thank Geoffry Laufersky and Thomas Nann in SCPS at VUW, as well as the Fan Group in ECE at HKUST and the Tang Group in the Department of Chemistry at HKUST for help with PLQY measurements. Special thanks to Matthew Cryer and David Flynn for their assistance.

■ ABBREVIATIONS

RP,Ruddlesden−Popper; BA,butyl ammonium; EQE,external quantum efficiency; PLQY,photoluminescence quantum yield

■ REFERENCES

(1) Chin, X. Y.; Perumal, A.; Bruno, A.; Yantara, N.; Veldhuis, S. A.; Martínez-Sarti, L.; Chandran, B.; Chirvony, V.; Lo, A. S.-Z.; So, J.; et al. Self-assembled hierarchical nanostructured perovskites enable highly efficient LEDs via an energy cascade. *Energy Environ. Sci.* **2018**, *11* (7), 1770−1778.

(2) Song, J.; Li, J.; Li, X.; Xu, L.; Dong, Y.; Zeng, H. Quantum Dot Light-Emitting Diodes Based on Inorganic Perovskite Cesium Lead Halides (CsPbX3). *Adv. Mater.* **2015**, *27* (44), 7162−7167.

(3) Li, J.; Xu, L.; Wang, T.; Song, J.; Chen, J.; Xue, J.; Dong, Y.; Cai, B.; Shan, Q.; Han, B.; et al. 50-Fold EQE Improvement up to 6.27% of Solution-Processed All-Inorganic Perovskite $CsPbBr_3$ QLEDs via Surface Ligand Density Control. *Adv. Mater.* **2017**, *29* (5), 1603885.

(4) Zhang, X.; Xu, B.; Zhang, J.; Gao, Y.; Zheng, Y.; Wang, K.; Sun, X. W. All-Inorganic Perovskite Nanocrystals for High-Efficiency Light Emitting Diodes: Dual-Phase $CsPbBr_3$-$CsPb_2Br_5$ Composites. *Adv. Funct. Mater.* **2016**, *26* (25), 4595−4600.

(5) Sun, C.; Zhang, Y.; Ruan, C.; Yin, C.; Wang, X.; Wang, Y.; Yu, W. W. Efficient and Stable White LEDs with Silica-Coated Inorganic Perovskite Quantum Dots. *Adv. Mater.* **2016**, *28* (45), 10088−10094.

(6) Protesescu, L.; Yakunin, S.; Bodnarchuk, M. I.; Krieg, F.; Caputo, R.; Hendon, C. H.; Yang, R. X.; Walsh, A.; Kovalenko, M. V. Nanocrystals of cesium lead halide perovskites ($CsPbX_3$, X= Cl, Br, and I): novel optoelectronic materials showing bright emission with wide color gamut. *Nano Lett.* **2015**, *15* (6), 3692−3696.

(7) Cho, H.; Kim, Y. H.; Wolf, C.; Lee, H. D.; Lee, T. W. Improving the Stability of Metal Halide Perovskite Materials and Light-Emitting Diodes. *Adv. Mater.* **2018**, *30* (42), 1704587.

(8) Deschler, F.; Price, M.; Pathak, S.; Klintberg, L. E.; Jarausch, D.-D.; Higler, R.; Hüttner, S.; Leijtens, T.; Stranks, S. D.; Snaith, H. J.; et al. High photoluminescence efficiency and optically pumped lasing in solution-processed mixed halide perovskite semiconductors. *J. Phys. Chem. Lett.* **2014**, *5* (8), 1421−1426.

(9) Yuan, M.; Quan, L. N.; Comin, R.; Walters, G.; Sabatini, R.; Voznyy, O.; Hoogland, S.; Zhao, Y.; Beauregard, E. M.; Kanjanaboos, P.; et al. Perovskite energy funnels for efficient light-emitting diodes. *Nat. Nanotechnol.* **2016**, *11* (10), 872−877.

(10) Hong, X.; Ishihara, T.; Nurmikko, A. Dielectric confinement effect on excitons in PbI_4-based layered semiconductors. *Phys. Rev. B: Condens. Matter Mater. Phys.* **1992**, *45* (12), 6961.

(11) Liu, J.; Leng, J.; Wu, K.; Zhang, J.; Jin, S. Observation of Internal Photoinduced Electron and Hole Separation in Hybrid Two-Dimentional Perovskite Films. *J. Am. Chem. Soc.* **2017**, *139* (4), 1432−1435.

(12) Dai, X.; Zhang, Z.; Jin, Y.; Niu, Y.; Cao, H.; Liang, X.; Chen, L.; Wang, J.; Peng, X. Solution-processed, high-performance light-emitting diodes based on quantum dots. *Nature* **2014**, *515* (7525), 96−99.

(13) Anikeeva, P. O.; Halpert, J. E.; Bawendi, M. G.; Bulovic, V. Quantum dot light-emitting devices with electroluminescence tunable over the entire visible spectrum. *Nano Lett.* **2009**, *9* (7), 2532−2536.

(14) Anikeeva, P. O.; Halpert, J. E.; Bawendi, M. G.; Bulović, V. Electroluminescence from a mixed red− green− blue colloidal quantum dot monolayer. *Nano Lett.* **2007**, *7* (8), 2196−2200.

(15) Kim, Y. H.; Cho, H.; Heo, J. H.; Kim, T. S.; Myoung, N.; Lee, C. L.; Im, S. H.; Lee, T. W. Multicolored Organic/Inorganic Hybrid Perovskite Light-Emitting Diodes. *Adv. Mater.* **2015**, *27* (7), 1248−1254.

(16) Si, J.; Liu, Y.; He, Z.; Du, H.; Du, K.; Chen, D.; Li, J.; Xu, M.; Tian, H.; He, H.; et al. Efficient and High-Color-Purity Light-Emitting Diodes Based on In Situ Grown Films of $CsPbX_3$ (X= Br, I) Nanoplates with Controlled Thicknesses. *ACS Nano* **2017**, *11* (11), 11100−11107.

(17) Wang, N.; Cheng, L.; Ge, R.; Zhang, S.; Miao, Y.; Zou, W.; Yi, C.; Sun, Y.; Cao, Y.; Yang, R. Perovskite light-emitting diodes based on solution-processed self-organized multiple quantum wells. *Nat. Photonics* **2016**, *10* (11), 699−704.

(18) Xiao, Z.; Kerner, R. A.; Zhao, L.; Tran, N. L.; Lee, K. M.; Koh, T.-W.; Scholes, G. D.; Rand, B. P. Efficient perovskite light-emitting diodes featuring nanometre-sized crystallites. *Nat. Photonics* **2017**, *11* (2), 108−115.

(19) Yang, X.; Zhang, X.; Deng, J.; Chu, Z.; Jiang, Q.; Meng, J.; Wang, P.; Zhang, L.; Yin, Z.; You, J. Efficient green light-emitting diodes based on quasi-two-dimensional composition and phase engineered perovskite with surface passivation. *Nat. Commun.* **2018**, *9* (1), 570.

(20) Quan, L. N.; Zhao, Y.; García de Arquer, F. P.; Sabatini, R.; Walters, G.; Voznyy, O.; Comin, R.; Li, Y.; Fan, J. Z.; Tan, H.; et al. Tailoring the Energy Landscape in Quasi-2D Halide Perovskites Enables Efficient Green-Light Emission. *Nano Lett.* **2017**, *17* (6), 3701−3709.

DOI: 10.1021/acs.chemmater.8b02999
Chem. Mater. 2019, 31, 83−89

(21) Gélvez-Rueda, M. C.; Hutter, E. M.; Cao, D. H.; Renaud, N.; Stoumpos, C. C.; Hupp, J. T.; Savenije, T. J.; Kanatzidis, M. G.; Grozema, F. C. Interconversion between Free Charges and Bound Excitons in 2D Hybrid Lead Halide Perovskites. *J. Phys. Chem. C* **2017**, *121* (47), 26566−26574.
(22) Cao, D. H.; Stoumpos, C. C.; Farha, O. K.; Hupp, J. T.; Kanatzidis, M. G. 2D homologous perovskites as light-absorbing materials for solar cell applications. *J. Am. Chem. Soc.* **2015**, *137* (24), 7843−7850.
(23) Smith, I. C.; Hoke, E. T.; Solis-Ibarra, D.; McGehee, M. D.; Karunadasa, H. I. A layered hybrid perovskite solar-cell absorber with enhanced moisture stability. *Angew. Chem.* **2014**, *126* (42), 11414−11417.
(24) Quan, L. N.; Yuan, M.; Comin, R.; Voznyy, O.; Beauregard, E. M.; Hoogland, S.; Buin, A.; Kirmani, A. R.; Zhao, K.; Amassian, A.; et al. Ligand-stabilized reduced-dimensionality perovskites. *J. Am. Chem. Soc.* **2016**, *138* (8), 2649−2655.
(25) Cheng, L.; Cao, Y.; Ge, R.; Wei, Y.-Q.; Wang, N.-N.; Wang, J.-P.; Huang, W. Sky-blue perovskite light-emitting diodes based on quasi-two-dimensional layered perovskites. *Chin. Chem. Lett.* **2017**, *28* (1), 29−31.
(26) Chang, J.; Zhang, S.; Wang, N.; Sun, Y.; Wei, Y.; Li, R.; Yi, C.; Wang, J.; Huang, W. Enhanced Performance of Red Perovskite Light-Emitting Diodes through the Dimensional Tailoring of Perovskite Multiple Quantum Wells. *J. Phys. Chem. Lett.* **2018**, *9* (4), 881−886.
(27) Kumar, S.; Jagielski, J.; Yakunin, S.; Rice, P.; Chiu, Y.-C.; Wang, M.; Nedelcu, G.; Kim, Y.; Lin, S.; Santos, E. J.; et al. Efficient blue electroluminescence using quantum-confined two-dimensional perovskites. *ACS Nano* **2016**, *10* (10), 9720−9729.
(28) Yao, E. P.; Yang, Z.; Meng, L.; Sun, P.; Dong, S.; Yang, Y.; Yang, Y. High-Brightness Blue and White LEDs based on Inorganic Perovskite Nanocrystals and their Composites. *Adv. Mater.* **2017**, *29* (23), 1606859.
(29) Hu, H.; Salim, T.; Chen, B.; Lam, Y. M. Molecularly engineered organic-inorganic hybrid perovskite with multiple quantum well structure for multicolored light-emitting diodes. *Sci. Rep.* **2016**, *6*, 33546.
(30) Liang, D.; Peng, Y.; Fu, Y.; Shearer, M. J.; Zhang, J.; Zhai, J.; Zhang, Y.; Hamers, R. J.; Andrew, T. L.; Jin, S. Color-pure violet-light-emitting diodes based on layered lead halide perovskite nanoplates. *ACS Nano* **2016**, *10* (7), 6897−6904.
(31) Shang, Y.; Li, G.; Liu, W.; Ning, Z. Quasi-2D Inorganic CsPbBr3 Perovskite for Efficient and Stable Light-Emitting Diodes. *Adv. Funct. Mater.* **2018**, *28*, 1801193.
(32) Li, G.; Rivarola, F. W. R.; Davis, N. J.; Bai, S.; Jellicoe, T. C.; de la Peña, F.; Hou, S.; Ducati, C.; Gao, F.; Friend, R. H.; et al. Highly Efficient Perovskite Nanocrystal Light-Emitting Diodes Enabled by a Universal Crosslinking Method. *Adv. Mater.* **2016**, *28* (18), 3528−3534.
(33) Wang, Q.; Ren, J.; Peng, X.-F.; Ji, X.-X.; Yang, X.-H. Efficient Sky-Blue Perovskite Light-Emitting Devices Based on Ethylammonium Bromide Induced Layered Perovskites. *ACS Appl. Mater. Interfaces* **2017**, *9* (35), 29901−29906.
(34) Niu, Y.-H.; Munro, A. M.; Cheng, Y.-J.; Tian, Y.; Liu, M. S.; Zhao, J.; Bardecker, J. A.; Jen-La Plante, I.; Ginger, D. S.; Jen, A. K.-Y. Improved Performance from Multilayer Quantum Dot Light-Emitting Diodes via Thermal Annealing of the Quantum Dot Layer. *Adv. Mater.* **2007**, *19* (20), 3371−3376.
(35) de Mello Donegá, C.; Liljeroth, P.; Vanmaekelbergh, D. Physicochemical Evaluation of the Hot-Injection Method, a Synthesis Route for Monodisperse Nanocrystals. *Small* **2005**, *1* (12), 1152−1162.
(36) Akkerman, Q. A.; Gandini, M.; Di Stasio, F.; Rastogi, P.; Palazon, F.; Bertoni, G.; Ball, J. M.; Prato, M.; Petrozza, A.; Manna, L. Strongly emissive perovskite nanocrystal inks for high-voltage solar cells. *Nat. Energy* **2017**, *2* (2), 16194.
(37) Stouwdam, J. W.; Janssen, R. A. Red, green, and blue quantum dot LEDs with solution processable ZnO nanocrystal electron injection layers. *J. Mater. Chem.* **2008**, *18* (16), 1889−1894.
(38) Vashishtha, P.; Halpert, J. E. Field-Driven Ion Migration and Color Instability in Red-Emitting Mixed Halide Perovskite Nanocrystal Light-Emitting Diodes. *Chem. Mater.* **2017**, *29* (14), 5965−5973.
(39) Yantara, N.; Bhaumik, S.; Yan, F.; Sabba, D.; Dewi, H. A.; Mathews, N.; Boix, P. P.; Demir, H. V.; Mhaisalkar, S. Inorganic halide perovskites for efficient light-emitting diodes. *J. Phys. Chem. Lett.* **2015**, *6* (21), 4360−4364.
(40) Huang, Y.; Yin, W.-J.; He, Y. Intrinsic Point Defects in Inorganic Cesium Lead Iodide Perovskite $CsPbI_3$. *J. Phys. Chem. C* **2018**, *122* (2), 1345−1350.
(41) Lin, C. C.; Meijerink, A.; Liu, R.-S. Critical red components for next-generation white LEDs. *J. Phys. Chem. Lett.* **2016**, *7* (3), 495−503.
(42) Eperon, G. E.; Paterno, G. M.; Sutton, R. J.; Zampetti, A.; Haghighirad, A. A.; Cacialli, F.; Snaith, H. J. Inorganic caesium lead iodide perovskite solar cells. *J. Mater. Chem. A* **2015**, *3* (39), 19688−19695.
(43) Wang, S.-W.; Lin, H.-Y.; Lin, C.-C.; Kao, T. S.; Chen, K.-J.; Han, H.-V.; Li, J.-R.; Lee, P.-T.; Chen, H.-M.; Hong, M.-H.; et al. Pulsed-laser micropatterned quantum-dot array for white light source. *Sci. Rep.* **2016**, *6*, 23563.

DOI: 10.1021/acs.chemmater.8b02999
Chem. Mater. 2019, 31, 83−89